Fire and vegetation dynamics in North-West Siberia during the last 60 years based on high-resolution remote sensing

Oleg Sizov[1,*], Ekaterina Ezhova[2,*], Petr Tsymbarovich[3], Andrey Soromotin[4], Nikolay Prihod'ko[4], Tuukka Petäjä[2,4], Sergej Zilitinkevich[2,5], Markku Kulmala[2,4], Jaana Bäck[6], and Kajar Köster[6]

[1]Institute of Oil and Gas Problems Russian Academy of Science, Moscow, Russia
[2]Institute for Atmospheric and Earth System Research (INAR)/Physics, University of Helsinki, Finland
[3]Institute of Geography Russian Academy of Science, Moscow, Russia
[4]Tyumen' State University, Tyumen', Russia
[5]Finnish Meteorological Institute, Helsinki, Finland
[6]Institute for Atmospheric and Earth System Research (INAR)/Forest Sciences, University of Helsinki, Finland
[*]These authors contributed equally to this work.

Correspondence: Ekaterina Ezhova (ekaterina.ezhova@helsinki.fi)

Abstract. Rapidly warming Arctic undergoes transitions that can influence global carbon balance. One of the key processes is the shift towards plant species with higher biomass underlining a stronger carbon sink. The shift is predicted by the models based on abiotic climatic factors but it is not always confirmed with observations. Here we use high-resolution remote sensing to study the process of transition of tundra into forest on the 20 000 km^2 area in North-West Siberia. Overall, 40% of the study area was burned during 60-yr period. Three quarters of the burned areas were dry tundra. Ca 10% of the study area experienced 2-3 fires with an interval of 15-60 years suggesting a shorter fire return interval than that reported earlier for the northern areas of Central Siberia (130-350 years). Based on our results, the shift in vegetation (within the 60-years period) occurred in 40-85% of the burned territories. All fire-affected territories were flat, therefore no effect of topography was detected. Oppositely, in the undisturbed areas, tundra-forest transition was observed only in 6-15% of the territories, characterized by steeper topographic slopes.Our results suggest a strong role of disturbances for the tree advance in North-West Siberia.

1 Introduction

North-West Siberia is the region subject to a strong warming trend in summer as compared to the Arctic average. The annual warming trend reported for the entire Arctic (data set from 1971-2017) is 0.6°C per decade, resulting from the cold season trend of 0.7°C per decade, and the warm season (June-September) trend of 0.4°C per decade (Box et al., 2019) in the Arctic as a whole. According to the 2nd Assessment report on the climate change on the Russian territory (Katsov et al., 2014), the winter warming trend in North-West Siberia (data set from 1972–2012) is 0.4-0.7°C per decade, which is comparable to the trends reported for the entire Arctic. However, the summer trend is 0.8-1.0°C higher per decade, double that is reported for the entire Arctic. At the same time, meteorological observations indicate that snow cover thickness increased at the rate 2-10 cm per decade but the number of snow cover days decreased at the rate up to 8 days per decade (Katsov et al., 2014). An increase in warm degree-days favors a shift of vegetation type towards more southern species, i.e., transformation of tundra

environment into shrubs and forest vegetation. The higher amount of biomass in the shrubs and trees will increase terrestrial carbon sink providing means for climate mitigation. Forest ecosystems can additionally enhance carbon uptake via complex atmosphere-biosphere feedback mechanisms (Kulmala et al., 2013; Kalliokoski et al., 2019).

Shrubification of tundra has been reported in many recent studies (Myers-Smith and Hik, 2018; Maliniemi et al., 2018; Bjorkman et al., 2020) and it has been associated with the greening of the Arctic (Myers-Smith et al., 2020). However, there is no general agreement regarding tree propagation. Modelling studies based on abiotic factors predict tree-line advance to the north (Tchebakova et al., 2010; Kaplan and New, 2006; Aakala et al., 2014). Nevertheless, this advance has been only partially confirmed by observations (Harsch and Bader, 2011) and observed rates are extremely low as compared to theoretical predictions (Van Bogaert et al., 2011). On the contrary, the study based on the forest inventories from the eastern United States shows that forested areas shrink rather than expand on most plots at their range limits (Zhu et al., 2012). These discrepancies suggest that there exist other factors than climatic ones influencing the transition. First, Frost and Epstein (2014) found transition of tundra to shrubs and trees to be dependent on another abiotic factor: topographic slope. Different topographic slopes result in different insolation, moisture regime and permafrost state. Second, it was hypothesized that the biotic factors have a significant effect together with the abiotic climatic factors (Woodward et al., 2004). Availability of seeds, germination success and presence of major species competing with newly establishing plants can all influence propagation of the tree-line. A recent study suggests that the shift of biomes occurs episodically and requires a disturbance (Renwick and Rocca, 2015). In northern latitudes (boreal, subarctic and arctic areas), wildfires and grazing by reindeer are the two main disturbances that really influence the vegetation structure and dynamics (Köster et al., 2013; Narita et al., 2015), which in turn induce shifts in ecosystem processes, e.g. nutrient cycles and ecological interactions.

The reindeer regulate the abundance of species and community composition via grazing. Both observations and field experiments in tundra show different response to warming with and without large herbivores (Post and Pedersen, 2008; Olofsson et al., 2009), manifested by enhanced growth of deciduous shrubs on the sites not affected by grazing. However, evergreen shrubs and trees demonstrate an opposite trend towards increased growth at the sites exposed to grazing (Bernes et al., 2015). The effect of wildfires on vegetation shift in tundra is less studied. Fire has been found to reduce the cover of lichens and bryophytes (Joly et al., 2009), but enhance the growth of grasses and shrubs (Barrett et al., 2012; Narita et al., 2015). Land-hausser and Wein (1993) observed that forests in the Canada's Northwest Territories advance in the forest-tundra ecotone after a strong wildfire. Long before that Sannikov et al. (1970) noted that seedlings survival is the highest on bare mineral soils, and high intensity and severity wildfires, which remove the organic material and expose mineral soil, can favor tree survival.

Here we study the shift in vegetation based on high-resolution remote sensing data, in the territory including southern tundra, forest-tundra ecotone and northern taiga in the Nadym-Pur district of North-West Siberia. Opposite to northerly-located Yamal and Gydan peninsulas and westerly-located Priuralsky district, this territory has not yet suffered from reindeer pasture overuse (Matveev and Musaev, 2013). Therefore, grazing could be of secondary importance for the ecosystem changes in these areas. We hypothesize, based on the study of Landhausser and Wein (1993), that forest expansion occurs mainly in the areas affected by relatively recent wildfires, while other areas (non-disturbed background areas) demonstrate only a minor change

in vegetation. Thus, we focus on the effect of wildfires on the vegetation, specifically on tundra-forest and tundra-woodlands transition. The main objectives of the study are:

1) to study dynamics of regional climatic factors in order to assess the possibility of vegetation shifts due to climate change, in particular tundra-forest transition;

2) to quantify burned surface areas and calculate frequency of wildfires;

3) to study the link between wildfires and dry tundra transition to woodlands and forests.

Finally, we take into account physiographic characteristics of the landscape and study the link between the topographic slope and the transition.

2   Materials and methods

2.1   Field sites

2.1.1   General description

In order to study tundra-forest transition, we selected the monitoring sites satisfying two predefined criteria:

1) the sites are covered by the archive Corona imagery (Ruffner, 1995);

2) the sites have projective forest cover less than 10% according to the Landsat forest mask (Hansen et al., 2013).

Based on these criteria, we identified three main study areas (Table 1, Fig. 1). Area 1 (the largest area) is located on the east coast of the river Nadym, area 2 is between the south coast of the Gulf of Ob' and river Yarudey and area 3 is to the west from the city of Nadym (Fig. 1). Detailed maps of study sites can be found in geoportal 'Nadym. Changes in 50 years (1968-2018) (NC50)' (https://ageoportal.ipos-tmn.ru/nadym/). Description of the geoportal is given in Appendix A.

Northern part of study area 1 is in the continuous permafrost zone, while its southern part and study areas 2 and 3 are in the discontinuous permafrost zone (Trofimova and Balybina, 2015). The vegetation zones include southern tundra, forest-tundra ecotone and northern taiga (Ilyina et al., 1985), with the treeline crossing the study sites (Walker et al., 2005; MacDonald et al., 2008). Southern tundra zone is represented by dwarf-shrub, moss and lichen tundra, polygonal peatlands and dwarf-shrub, lichen woodlands. Vegetation community of the forest-tundra consists of larix and spruce-larix, dwarf-shrub moss woodlands and dwarf-shrub lichen tundra. Northern taiga is represented by larix and spruce-larix dwarf-shrub and moss-lichen forests and shrub-moss-lichen wetlands in flat or hilly terrain. The boundaries of these vegetation zones in the study areas, according to Ilyina et al. (1985), are shown in Fig. 1.

In addition, Fig. 1 shows the forest mask derived from the topographic map by Ilyina et al. (1985). Forested areas include dense forests, shrubs in the floodplains and river deltas, forest sprouting. Overall, 3570 km^2 or 17.5% of the total study area was covered by forests, with 15.5% covered by dense forest, 1.2% covered by forest sprouting and less than 1% covered by shrubs. Dry tundra ('moss and lichen tundra' in the topographic map) covered 11 370 km^2 or 55.7% of the total study area.

The anthropogenic activity in the study areas includes oil and gas mining (fields Medvezhye and Yarudeyskoe, major gas pipelines Yamburg-Tula, Yamburg-Yelets, SRTO-Ural, Urengoy-Center, Urengoy-Uzhgorod). The first geological surveys

started in 1950s and the industrial exploration of the area started in 1967. New railway road 'Northern Latitudinal Railway' (Salekhard-Novy Urengoy) is currently under construction within study area 1. Environmental impact due to anthropogenic activities and climate change has been monitored since 1970s (Matyshak et al., 2017a, b; Sizov and Lobotrosova, 2016; Kukkonen et al., 2020).

2.1.2 In-situ observations of vegetation and permafrost state

In August 2019, a field campaign was performed near Pangody in the central part of study area 1 (Fig. 1) to study vegetation cover and state of permafrost. We chose three sites: one in the background area, one in the area burned before 1968 and one in the area burned in 1968 and 1988. Photos from two of them are shown in Fig. 2. The land cover of each site consisted mainly of mosses, grasses and shrubs (detailed classification is given in Table 2), and the major tree species were larix and spruce (*Larix sibirica, Picea obovata*). In the burned sites, birch (*Betula pendula*) and pine (*Pinus Sylvestris L.*) were also observed.

The active layer thickness (the depth of annual thaw) was measured using a metal rod: the rod was pushed vertically into the ground until it reached frozen soil. Active layer thickness (ALT) for three sites is reported in Table 2.

2.2 Calculation of climatic indices

In order to assess the climatic conditions in the region, we used meteorological data (http://meteo.ru, latest access July 2019) from three stations, Nadym, Nyda and Novy Port (Supplementary material, SM), located along a 200 km latitudinal transect from the south (65.3N, Nadym) to the north (67.4N, Novy Port). Station Nadym (65°32'N, 72°32'E, 7 m a.s.l.) is located near the southern borders of the study areas (50 km from study area 3). Station Nyda (66°37'N, 72°57'E, 10 m a.s.l.) is located within study area 1. Station Novy Port (67°41'N, 72°52'E, 12 m a.s.l.) is located to the north of the study areas. This is the closest station to the northern boundaries of the study areas. The data set contained 52 years of quality-checked meteorological observations (from 1966 to 2018), including air temperature (time resolution 3 h), precipitation (time resolution 12 h), and cloudiness 0 to 10 (time resolution 3 h). Based on this data set, we calculated the mean monthly temperatures (the sum of daily mean temperatures divided by the number of days in a month), monthly cumulative precipitation (the sum of daily precipitation measurements for a given month), the daily minimum and maximum temperatures for all the years.

In order to assess climatic factors influencing vegetation dynamics, we studied the length and mean temperature of the growing season, which we define as the period with daily mean temperatures above +5°C (Tchebakova et al., 1994). We calculated growing degree-days following Tchebakova et al. (1994),

$$GDD_5 = \sum_{\overline{T} \geq 5} (\overline{T} - 5), \tag{1}$$

where $\overline{T}$ - is the daily mean temperature [°C]. Another important abiotic factor for vegetation is humidity. We calculated potential evapotranspiration (PET) from the temperature and cloudiness measurements using Bonan's modification (Bonan, 1989) of Taylor-Priestley model (Priestley and Taylor, 1972). We used PET and precipitation to calculate a dryness index (DI)

(Tchebakova et al., 1994), i.e. the ratio between annual PET and precipitation (P):

$$DI = \frac{PET}{P}. \tag{2}$$

Based on GDD$_5$ and DI, we classified vegetation zones in Nadym, Nyda and Novy Port using the thresholds by Tchebakova
et al. (1994) (see Table 3). Due to the fact that the stations are located along the latitudinal transect close to the study sites, they
should be representative of their vegetation state.

2.3 Wildfires

The initial state of the study areas was assessed using Corona images. We identified 21 frames under clear-sky conditions
from 21 August 1968. Each frame consisted of 4 scanned fragments. The cropped fragments without color correction were
georeferenced to the chosen orthomosaic (SPOT layer, sec. 2.4) using polynomial method (3rd order) in software ArcGIS (v.
10.4.1). The r.m.s. error of georegistration estimated using control points did not exceed 10-12 m. Then the fragments were
organized in separate paths and finally a mosaic was formed using mosaic operator Last in ArcGIS. This mosaic characterized
the state of study areas before the active industrial exploration of the region (started in 1967).

Further, we used Landsat data to quantify burned areas. The data providing the best coverage of the study areas were available
from the following years: 1988, 2001, 2016 and 2018 (Table 4). The images were synthesized using near- and mid-infrared
channels (Landsat 5 and 7: 0.63-0.69 μm, 0.76-0.90 μm and 1.55-1.75 μm; Landsat 8: 0.64-0.67 μm, 0.85-0.88 μm and 1.57-
1.65 μm) as burned areas are visible in the infrared range of wavelengths. Landsat mosaics for all years were formed with
application of color correction using mosaic operator Blend in ArcGIS.

Mapping and quantification of the burned areas were performed by means of an object-based image analysis, successfully
used for studies of landscape dynamics (Blaschke, 2010). On the first stage, we performed segmentation of mosaics using
algorithm 'Multiresolution segmentation' in software eCognition (v. 9.0). The segmentation was done using parameters 40 for
Scale and 0.5 for Color. The second stage, classification, was different for Corona and Landsat mosaics. For Landsat mosaics,
we used unsupervised classification ISODATA (15 classes, a change threshold 5%). Further, we identified visually one or two
classes corresponding to burned areas. The segments containing more than 90% of pixels within these classes were identified
as burned areas. In addition, we checked the segments with lower percentage of pixels (down to 40-50%) belonging to these
classes and they were manually added to burned areas when necessary. In Corona mosaics, the spectral information was missing
and we had to rely on the contrast of colors between background tundra and burned areas. For visual classification we applied
two criteria. First, background tundra is lighter due to the presence of lichen in vegetation community, whereas recently burned
areas are dark. Second, burned areas are characterized by well-defined boundaries often coinciding with river coastlines. An
example illustrating segmentation and the visual choice of burned areas is shown in Fig 3. Calculation of the areas of segments
classified as burned areas was performed using standard instrument Calculate geometry in ArcGIS.

We studied the percentage and distribution of the burned sites and calculated the frequency of fire return. Corona and Landsat
images showed that some years were characterized by particularly large-scale fires in the study areas (see an example for 1990
in SM, Fig. SB1). These years are referred to as the years of major fires. The burned areas can be detected in the satellite

150   images during a few years after the fire. Landsat mosaics from 1988, 2001, 2016 and 2018 largely reflect the state of the study areas after the major fire years 1976, 1990, 2012 and 2016 (Table 5). Burned areas in Corona mosaic from 1968 were partially dated back to the fires in the period 1953-1964 based on geological surveys and early Corona images (the sources are listed below Table 5). For a given territory, the period between fires was calculated as the difference in years between the major fires.

2.4   Vegetation dynamics

155   To monitor vegetation dynamics, we visually compared the data from archive imagery from the Corona mission (Ruffner, 1995) and topographic maps to the state-of-the-art satellite data of super high resolution (SPOT-6,7, Resurs-P 1-2). The data sets are summarized in Table 6. A similar visual method was used by e.g. Frost and Epstein (2014) to study transition from grassland to shrubs in northern Eurasia.

     The initial state of vegetation was obtained from Corona imagery and topographic maps. The compilation of mosaic using
160   Corona images is described in Section 2.3. The topographic maps were used to develop forest and dry tundra masks using automatic tracing in software EasyTrace (v. 8.7). The resulting vector layer was checked and corrected using Corona mosaic.

     Assessment of the current state of vegetation was based on Resurs-P and SPOT data (Table 6). Majority of the territory was covered by mosaic of SPOT-6,7 imagery synthesized in the visible range without alignment of colors. Ca 10% of the territory were covered by three paths of Resurs-P (the product level 2A, including four channels B, G, R and NIR). The SPOT mosaic
165   was used as a pluggable webmap layer without additional processing. We co-registered Resurs-P data to the SPOT mosaic in ArcGIS.

     We studied the tundra-forest shift of dry tundra burned before 1968 and of background tundra (not affected by fires) during the period of ca 60 years. Firstly, based on the topographic map and Corona mosaic, we determined dry tundra areas burned before 1968 (Sec. 2.3) and not affected by fires during the whole study period. The area of burned tundra in the Corona mosaic
170   from 1968 was 1090 km^2, the area of background tundra was ca 5300 km^2. Then we introduced random sample circles with 100 m diameter within the subsets. The samples were spaced at intervals of 2 km within the burned areas (157 samples) and 5 km within background dry tundra (231 sample). Then we visually compared the areas inside the circles in the old and modern images (see examples in Fig. 4). We chose only those circles, for which we could confidently state that there was tundra and no trees in 1968. We focused on the vegetation shift after relatively 'old' fires (i.e., before 1968) because mature
175   trees, unambiguously distinguished in the satellite images, had higher chances to develop during ca 60 years. Furthermore, we visually separated woodland (trees covered less than 50% of the area inside the circle) and forest (trees covered more than 50% of the area inside the circle). For later fires, similar tundra-forest transition could also be expected, but visual analysis of younger trees is more challenging. Another issue is the lack of information on the vegetation state before more recent fires. Therefore, the analysis of vegetation shift after more recent fires was not performed.

180   In addition, we assessed the current state of vegetation with different times after the last fire using Normalized Difference Vegetation Index (NDVI). The index reflects the state of biomass, i.e. vegetation greening, density and development (Walker et al., 2003; Johansen and Tømmervik, 2014; Miles and Esau, 2016). NDVI was calculated from the visible (VIS) and near-

infrared (NIR) radiation reflected by vegetation:

$$NDVI = \frac{NIR - VIS}{NIR + VIS}.$$ (3)

185   NDVI was calculated based on two scenes from one path of Landsat-8 from 30 June 2018 (path/row 160/013 and 160/014). We used Level 2 data (CEOS) after atmospheric correction by the standard Landsat 8 OLI atmospheric correction algorithm (Vermote et al., 2016). NDVI was calculated in ArcGIS using standard tools.

     We calculated NDVI distributions for study area 1, separately for tundra burned in different years (as detected in satellite imagery mosaics from 1968, 1988, 2001, 2018) and for background tundra. In this analysis, we considered the territories

190   covered by one satellite flight burned only once in ∼60 years. In order to make the study areas more balanced by size, we merged the data sets from the burned territories detected in 1968 and 1988, for which we might expect that vegetation had recovered after the fires, and omitted 2016 due to insufficient size of the fire-affected territory. As a result, all study areas were larger than 600 km^2 (1968+1988 – 600 (405+195) km^2, 2001 – 1565 km^2, 2018 – 867 km^2, background – 937 km^2). Using the dates of major fires (Table 5) and the date of Landsat mosaic (2018), we can assume that NDVI within burned tundra sites

195   detected in 1968 and 1988 reflect the state of vegetation after fires more than 42 years ago, in 2001 – after fires 28 years ago, in 2018 – after fires 2 years ago. NDVI in background tundra refers to tundra not affected by fires during the whole study period.

2.5   Topographic slopes

To quantify the topographic slopes, we used a digital elevation model ArcticDEM (Table 6). The model is a mosaic with high spatial resolution (2 m). The stereo-couples for this version of the model were prepared in 2010-2017. It is currently the most

200   detailed source of information on the relief. Co-registration of mosaic elements, calculation of slopes and preparation of the raster layer for the geoportal NC50 (Appendix A) was done in ArcGIS.

     We calculated topographic slopes within the circles where we visually assessed the vegetation shift. For calculation, we used the circles with 50 m diameter located in the centers of larger circles. For each circle, we calculated mean slopes. We separated the data corresponding to burned and background states and further stratified it by vegetation shift ('no shift', 'to woodland',

205   'to forest'), thus splitting the data into 6 classes. Finally, we calculated the median values, 25th and 75th percentiles of mean slopes for each class.

3   Results

3.1   Temperature, precipitation and climatic indices

The mean monthly temperatures were above zero ca 4 months per year (June-September) in Novy Port and ca 4-5 months

210   per year in Nadym (May-September) (SM, Fig. SA1). The coldest month was January with the mean monthly temperature -23...-24°C, and the warmest month was July with +11...13°C.

     During the last 50 years, the mean annual temperature at the meteorological stations has increased by 2.6-3.0°C (Fig. 5). In addition, the daily minimum temperature has increased by 4-5°C (from -44...-45°C to -40°C, SM, Fig. SA2-SA4), whereas the

daily maximum temperature has increased significantly ($p < 0.05$) only in Novy Port, by 3.5°C (from 18 to 21.5°C, SM, Fig. SA2-SA4).

The length of the growing season (SM, Fig. SA2-SA4) has increased by 24 days: from 72 to 97 days in the north (Novy Port) and from 97 to 121 days in the south (Nadym). The mean temperature has increased by 1.0-1.4°C. In general, both the length and the mean temperature of the growing season exhibit great variability particularly during recent years. Following the mean temperature and the length of growing season, the growing degree-days, GDD_5, have increased over the last 50 years (Fig. 5). The strongest increase in GDD_5 (ca 200°C days) was observed during 20 years from 1966 to 1985, after which GDD_5 levelled off. The period from 1980 to 1995 seemed to be the most favorable period for a new forest establishment due to the relative stability of mean temperature and GDD_5. On the contrary, the last decade was characterized by a strong variability in both mean annual temperature (the peak-to-peak value was ca 3°C) and GDD_5 (the peak-to-peak value was larger than 400°C days), which could make seedlings' survival less probable.

Mean annual precipitation decreases from the south to the north: from 510 mm in Nadym to 330-340 mm in Novy Port (SM, Fig. SA1). Monthly variability of precipitation follows a well-pronounced seasonal cycle with a maximum in August (July-August in the south). Precipitation cycle in the southern part (Nadym, Fig. 6, SM, Fig. SA1) is characteristic of the temperate continental regime (Chorley, 1971), whereas precipitation in the northern part (Novy Port, Fig. 6, SM, Fig. SA1) is characteristic of the arctic regime with the annual precipitation below 400 mm. While the seasonal cycle of precipitation was similar in three stations, the inter-annual variability was not. Precipitation time series in Nyda and Novy Port were closely following each other between 1965 and 2005 (Fig. 6). Since 2005, the annual precipitation has increased in Nyda and it has drastically decreased in Novy Port. Potential evapotranspiration increased in all three sites. Accordingly, the dryness index (DI) increased from 0.4 to 0.5-0.6 everywhere (SM, Fig. SA5). During a few recent years, DI in Novy Port exceeded unity several times.

Based on the observed growing degree-days and the dryness index, the modelled vegetation class in the Novy Port has changed from forest-tundra to dark needled northern taiga, in Nadym – from dark needled northern taiga to dark needled middle taiga. The vegetation class in Nyda remained dark needled northern taiga (Table 3). The vegetation shift at two sites results from an increase in GDD_5, while DI was not a limiting factor for vegetation at any of the three stations. Due to the fact that GDD_5 is a function of air temperature and the latter depends mainly on latitude, GDD_5 from the three stations should be representative of our study areas. Therefore, we can conclude that heat and humidity throughout our study areas are theoretically suitable for forests.

3.2 Dynamics of fires

Weather conditions in Northern Siberia can support large-scale wildfires during summer time. The fires occur mainly in July (Ponomarev et al., 2016). Burned areas according to satellite imagery from 1968-2018 and reflecting the state of the areas after five major fire events (Table 5) are shown in Fig. 7a. The burned areas in Fig. 7a can overlap if the same site experienced more than one fire. Separate maps of the burned sites for each of five cases (Table 5) are available in geoportal NC50 (Appendix A).

The overall area of burned sites was ca 8300 km^2 constituting more than 40% of the total study area. Fig. 7b shows the distribution of the fraction of burned area over years. The largest fires, contributing more than 30% to the total burned area, occurred between 1989 and 2001 (mainly in 1990, Table 5, Fig. SB1). The fires in each of the periods 1953-1968, 1968-1988 and 2016-2018 contributed 10-20% of the total burned area (Fig. 7b). In addition, ca 10% of that area was recognized both in 1988 and 2001 imagery. According to Fig. 7b, ca 80% of the burned area experienced fire once and 20% experienced fires more than once during 60 years. Approximately 17% of the fire-affected territory (1400 km^2) burned twice, 2.5% of the territory (200 km^2) burned three times and 0.2% (20 km^2) burned four times. These sites were characterized by a remarkably small period between consequent fires, which was estimated as 15-60 years if only major fires were taken into account (Table 5).

3.3 Vegetation dynamics and its link to fires and topography

3.3.1 Assessment of vegetation recovery after fire using Normalized Difference Vegetation Index (NDVI)

Fig. 8a shows study area 1 with marked dry tundra burned in different time periods and marked dry background tundra. Fig. 8b shows the corresponding distributions of NDVI. As discussed in Methods (Sec. 2.4), 1968+1988 data reflect the state of vegetation in the site burned more than 42 years ago, 2001 data – 28 years ago, 2018 data – 2 years ago and background data refer to tundra not affected by fires during the whole study period.

In Fig. 8b, the NDVI distributions from the background tundra and recently burned sites are close to Gaussian ones. Interestingly, the distributions from the sites burned 28 and >42 years ago are bimodal and they have higher NDVI values as compared to the background and recently burned sites. We fitted the distributions by the sums of two Gaussian functions (the fits are shown in Fig. 8b) and determined mean values and standard deviations for all the peaks (Table 7). The positions of the lower peaks of the bimodal distributions differ only slightly, whereas the position of the upper peak is a bit lower and the peak is less pronounced for the distribution from the site burned 28 years ago.

Further, we used the mean values and standard deviations of the fitted Gaussian functions to identify vegetation associated with the peaks of the distributions. For illustration, we chose an image containing all representative examples of vegetation (Fig. 9). Green color in Fig. 9, right panel, indicates the pixels with NDVI in the interval (NDVI$_{max,2}$-σ_2; NDVI$_{max,2}$+σ_2) corresponding to the upper peak of the distribution based on the data from 1968+1988. Comparing left panel and right panel of Fig. 9, one can conclude that this peak is mainly associated with forest. The lower peak (pixels in blue color in Fig. 9, right panel) corresponds to woodlands and tundra. This lower peak has a large intersection with the peak in the unimodal distribution from the background site. However, interestingly, there is a significant decrease in the pixels with NDVI below ca 0.52 in the bimodal distributions. These pixels are marked in pink in Fig. 9, right panel. They correspond to the tundra sites lightest in color due to the presence of lichen in the vegetation community. The fraction of such pixels decreases in the bimodal distributions, meaning that lichen does not recover to its state before the fire. Instead, the bimodal distributions have a large fraction of pixels with high NDVI corresponding to forests, which are absent in background tundra.

Finally, we estimated the fraction of 'forest' pixels in the bimodal distributions. Using standard deviations of the two peaks, the boundary separating the forest peak from the tundra peak is NDVI = 0.72. We assumed that pixels with NDVI > 0.72

represent mainly forest, and pixels with NDVI < 0.72 – mainly tundra and woodlands. We integrated the bimodal distributions to find the fraction of pixels with NDVI > 0.72 in the total number of pixels. Our estimates show that in the areas burned 28 years ago, forests occupy 19% of the total area. In the areas burned more than 42 years ago, the fraction of 'forest' pixels increases to 28% of the total area.

While precise calculations of the forest fraction based on NDVI are challenging, the main results following from Figs. 8, 9 can be summarized as follows:

1. The NDVI distributions based on the data from background tundra and areas burned 2 years ago are predominantly unimodal, whereas the distributions based on the data from the areas burned 28 years ago and earlier are bimodal.

2. The low-NDVI pixels corresponding to vegetation communities in tundra with relatively high amounts of lichen and thus having the lightest colors in the images almost disappear from the distributions calculated for the vegetation communities recovered after fires.

3. Instead, the new state of vegetation recovered after fires is characterized by a higher mean NDVI due to the new peak associated with forest. The fraction of high-NDVI pixels representing forest increases with time after the last fire.

3.3.2 Assessment of vegetation shift using visual method, connection to fires and topography

Fig. 10 shows the results of the visual analysis of vegetation shift within dry tundra burned before 1968 (Sec. 3.3.1). The largest part of burned tundra was in the northern taiga zone, and relatively large part was in the forest-tundra ecotone. The burned area in southern tundra contained only 7 samples, therefore the corresponding results are not statistically reliable. The shift of vegetation indicated by green symbols is clearly seen in the forest-tundra, while it is less pronounced in the northern taiga.

Statistics of the shift is summarized in Table 8 and illustrated in Fig. 11. In the absence of disturbances, only a tiny fraction (ca 5%) of southern tundra exhibited vegetation shift from dry tundra to woodlands, whereas a somewhat larger proportion (15%) of changing vegetation was observed in the forest-tundra and northern taiga (Table 8). Note that none of the background dry tundra sites developed forest. On the contrary, burned dry tundra exhibited a significant shift towards tree-dominated vegetation: 85% of samples in the forest-tundra and 45% of samples in the northern taiga. More than 50% of samples showed change to forest in the forest-tundra ecotone (Table 8), and more than 10% of samples - in the northern taiga.

Finally, we assessed the link between the vegetation shift and topographic characteristics (Fig. 12). Our results show that there was a dependence on topography in the background areas. The median value of the mean topographic slope was ca one degree in the areas with no detected shift, ca three degrees in the areas with the shift towards woodlands, and it increased to six degrees in the areas with the shift towards forest. Note that there were only five points in the background areas with shift to forest, all of them were located in the river valleys (these points were not accounted in the statistics in Table 8). Oppositely, the slope dependence was weak or absent in the predominantly flat burned areas.

4 Discussion

Different climate models generally agree that the greatest warming due to the enhanced greenhouse gas emissions occurs at northern high latitudes (Sand et al., 2016). Studies show that the snowmelt and spring recovery occurs earlier in the Northern Hemisphere boreal and subarctic forest zone with a trend of two days per decade (Pulliainen et al., 2017), having a considerable effect on vegetation, but also on wildfire dynamics. At our sites, the length of growing season has a trend of 4.5-4.8 days per decade and the mean temperature of growing season is increasing by 0.2-0.3°C per decade (SM). Since 1966 the growing season temperature has increased by approximately 1°C, and the growing season has become longer by approximately 20 days. The cumulative heat index, growing degree-days (GDD_5), has increased by 200-300°C days. According to the calculated climatic indexes - GDD_5 and dryness index (DI) - conditions throughout the study areas are already suitable for forest and the treeline could have moved to the north. Interestingly, the strongest increase in GDD_5 was observed between years 1966 to 1985, followed by a stable period during the 80s and 90s, and this period was the most favorable to the trees to take over the tundra areas.

Besides atmospheric heat and moisture, the Arctic vegetation is sensitive to underlying permafrost. Myers-Smith et al. (2019) emphasized the importance of the increased ALT in addition to summer temperature and the elongated growing season for the vegetation shift based on the observations in the Canadian Arctic. They reported a change in a vegetation community composition, namely an increase in shrubs and graminoids, driven by climatic factors alone (see also Barrett et al., 2012; Narita et al., 2015). Tchebakova et al. (2010) suggested that for survival of tree species *Larix siberica* and *Picea obovata*, native to West Siberia, the active layer thickness (ALT) should exceed 1.5 m. Matyshak et al. (2017b) reported ALT of 58-70 cm in the peatlands near Nadym in 2007-2008, whereas Kukkonen et al. (2020) found ALT of 1-3 m in the nearby boreholes in 2009-2017. Our measurements (Sec. 2.1.2), although by no means extensive, show that the ALT is 40 cm in the background site and 1.5 m in the sites affected by relatively old fires (40 years ago) within study area 1. Due to the changes in surface energy balance, the ALT regularly increases within the first few years following fires (both in forest and tundra ecosystems), and ALT in the burned sites may be larger than in the unburned sites for two or three decades (Rocha and Shaver, 2011; Köster et al., 2018). Deeper ALT provides more space for tree roots, implying more favorable conditions for trees.

In addition, wildfires create new recruitment opportunities (Bret-Harte et al., 2013; Mekonnen et al., 2019). Combusting the vegetation and part of the organic soil layer, the fires create open patches on the soil, where pioneer species can start to grow. Moreover, the burned tundra is darker than the unburned area, which can accelerate tree establishment due to warmer conditions in the soil. This is supported by nutrients released by the burning biomass. Camac et al. (2017) found out that the fires increase shrub seedling survival by as much as 33-fold while warming positively affects their growth rates.

During the latest 60 years, the study sites experienced extensive fires burning 40% of the total territory. The distribution of burned sites among the study areas 1, 2, and 3 was not homogeneous. Within study area 1, a higher fraction of burned areas was detected (Fig. 7). Given the similarity of climatic conditions, a possible explanation is difference in anthropogenic activity. Oil and gas infrastructure within the areas 2 and 3 was launched only recently, whereas geological prospecting within the area

1 started already in 1967, major construction of infrastructures was performed in 1971 and exploitation of Medvezhye field
345 started in 1977. In our analysis of vegetation dynamics, we focused on study area 1 most affected by fires.

The time since last fire is an important parameter for the assessment of vegetation state. Within the study areas, the interval between the large-scale fire events, when more than 500 km^2 was burned, was 15-25 years. Using the current state of NDVI in the areas affected by fires, we estimated the time of vegetation recovery. The peak NDVI values in the sites that burned 28 years ago (Fig. 8, Table 6) exceeded the peak background NDVI value. The peak NDVI value in the sites that burned 2 years
350 ago was smaller than that of the background site. This suggests that the post-fire vegetation recovery in our study areas took 2-28 years. Landhausser and Wein (1993) studied recovery of vegetation after the strong fire in the field conditions. Within 5 years after the fire, 65% of the area was not recovered bare ground, but 22 years after the fire the area was fully recovered, which is in general agreement with our results.

The shift of NDVI distribution towards larger NDVI values was found in the sites that burned more than 28 years ago
355 suggesting that recovered vegetation is characterized by a larger amount of biomass, presumably due to the shift in species. The field campaign (Sec. 2.1.2) revealed an increase of the fraction of green mosses and the tree species (e.g. birch) typical for succession in the burned sites. Increased biomass due to change in vegetation state (increased population of shrubs and forests) after fires is consistent with the other studies (Landhausser and Wein, 1993; Barrett et al., 2012; Narita et al., 2015). Different studies underline bigger post-fire changes in the biomass and composition of the non-vascular plant community in tundra areas
360 (Lantz et al., 2013; Jones et al., 2013), compared to the vascular plant community (Landhausser and Wein, 1993) and in these conditions lichen biomass could take decades to centuries to recover.

Our results (sec. 3.3) suggest that the disturbances have an important effect on the forest advance. We observed an increase in the forest and woodland cover in the areas affected by relatively 'old' fires (60 years period). In undisturbed conditions, forest took over tundra vegetation on the slopes and in the river valleys. As tundra turned into woodlands on rather moderate
365 slopes (3 degrees), it is not likely that landslides played a definitive role. Instead, the vegetation shift may be related to the difference in insolation or hydrological regime (Walvoord et al., 2019). Frost and Epstein (2014) studied expansion of larch and tall shrubs in Siberia based on remote sensing. The expansion of trees and shrubs was observed in uplands, which were defined as the sites with topographic slopes above 2 degrees. This is in agreement with our findings. Notably, the topography was not an important factor for the vegetation shift in the fire-affected areas.

370 Finally, it is interesting to note that ca 20% of the burned territories experienced multiple fires with the intervals between consequent fires of 15-60 years. Compared to our results, the fire return interval in Siberian forests at similar latitudes but further to the east (100E), is 130 - 350 years (Kharuk et al., 2011). Note that Kharuk et al. (2011) studied a remote site, where typically lightning ignites the fire. Oppositely, our results suggest that the fire return period in the same latitudes can be significantly reduced, presumably due to anthropogenic influence. Concurrently, this effect could be amplified by higher
375 temperatures and enhanced evaporation. Note that according to Fig. 6, the years of major fires (1976, 1990, 2012 and 2016) were characterized by peaks in potential evapotranspiration, as well as by anomalously high temperature during the growing season (SM, Fig. SA2-SA4) exceeding the mean value by 1°C. Causes of fires in North-West Siberia will be the topic for the future research.

5 Conclusions

Conventional forest masks that are used in satellite data analysis do not work well in the forest-tundra areas and therefore cannot be used to assess shifts from tundra to forest. We used topographic maps and high-resolution remote sensing to study vegetation dynamics in the forest-tundra zone of North-West Siberia during the last 60 years. We found that the vegetation shift from dry tundra to forest was strongly associated with fires. In the background sites experiencing no fires, only 6% of the area in southern tundra developed some trees during the 60-year period. This number increased up to 15% of the area in the forest-tundra ecotone and northern taiga. The shift in the background area was sensitive to topography, and trees appeared mainly on the moderate slopes. In the fire-affected sites, after the same period, the tree-dominated vegetation occupied already 40-85% of the previous dry tundra in the forest-tundra ecotone and northern taiga.

Given the importance of the fires for the tundra-forest dynamics, we calculated fire frequency within the study area. The major fires, burning $600 - 2500$ km^2 of the study area, occurred every 15-25 years. Most of the burned area experienced fires only once during 60 years, although some parts experienced multiple burning, up to 4 times. For ca 1700 km^2 of the study area, the period between the consequent fires is rather short, ca 15-60 years. This was a much shorter period compared to the neighboring remote sites of Central Siberia (fire return period longer than 100 years) that are less affected by anthropogenic influence.

Monitoring of wildfires in Russia is focused on forests whereas importance of tundra fires is underestimated. This is a major overlook which might have great economic consequences taking into account that tundra fires further decrease pasture areas for reindeer, already extremely overused in North-West Siberia (by 100-150% on Yamal and Gydan peninsulas according to Matveev and Musaev, 2013). In our study sites, the fires burned half of the dry tundra (6000 km^2) in 60 years. As concluded from our analysis, most of these areas likely shifted or will shift to woodlands and forests.

Converting the tundra to dark needle leaved forest causes an energy balance shift where especially areas with spruce have a positive (warming) feedback to climate in the future. Decrease in albedo causes increase of energy input to the surface, and partitioning of energy shifts towards sensible heat flux at forested sites (Beringer et al., 2005).

On the positive side, increase of forest areas may give a hint to enhancement of carbon sink and accordingly also of Carbon-Sink+ (Kalliokoski et al., 2019). Overall, the importance and need of detailed comprehensive long-term data is also obvious, therefore it is important to complete and verify satellite remote sensing data by observations – to establish Station for Measuring Earth surface – Atmosphere Relations (SMEAR) (Kulmala, 2018) in North-West Siberia as a part of Pan-Eurasian Experiment (PEEX) activities (Kulmala et al., 2015; Lappalainen et al., 2016; Petäjä et al., 2020).

Code and data availability. Meteorological data are available on the following website: http://meteo.ru. Study areas, reference sites, burned areas and control points for vegetation change can be found in geoportal NC50 (https://ageoportal.ipos-tmn.ru/nadym/). Other data sets are available from the authors upon request.

Appendix A: Description of geoportal 'Nadym. Changes in 50 years (1968-2018)' (NC50)

The geoportal 'Nadym. Changes in 50 years (1968-2018)' (NC50), available at https://ageoportal.ipos-tmn.ru/nadym/, aims to provide detailed geographical information on the study sites. There are three maps in geoportal NC50 (Fig. A1). The maps are synchronized, i.e. zoom or pan in one of the maps results in the same operation in two other maps. Each map contains a pointer in the center.

1) Map 1 is constructed of Corona/KH-4b imagery with marked study areas and reference sites. In the upper left corner, there are zoom instruments. In the upper right corner, there is a widget containing bookmarks of the reference sites. The reference sites are marked by yellow polygons in the map 1.

2) Map 2 is constructed of super high-resolution imagery: Yandex Maps, Bing Maps or Global Forest Watch. Fire-affected areas from different years can be overlain on this map. In addition, the field of Map 2 can be used to check the vegetation change in the control points. In the upper right corner, there is a panel of map layers.

3) Map 3 can be used as a digital elevation map (ArcticDEM) or a topographic map. In the upper right corner, there is a panel of map layers and coordinates of the pointer position (degrees-minutes-seconds). The coordinates in the decimal format are copied to the clipboard by a mouse click.

Author contributions. EE, OS and KK designed and conceptualized the study. OS and PT developed the geoportal, analyzed the data, prepared figures and interpreted results. NP performed on-site data acquisition. EE analysed the data, prepared figures, interpreted results and wrote the manuscript. KK interpreted results and contributed to writing discussion. AS, KK, JB, TP, SZ and MK contributed with data interpretation and writing - review and editing. All the authors commented on the manuscript.

Competing interests. The authors declare that they have no conflict of interest.

Acknowledgements. EE and TP acknowledge Academy of Finland Center of Excellence program (grant no. 307331) and Belmont Forum project Arctic Community Resilience to Boreal Environmental change: Assessing Risks from fire and disease (ACRoBEAR) via Academy of Finland, decision number 334792. OS and AS were funded by RFBR, research project 20-55-71004. PT was funded by Russian Science Foundation project 18-17-00178. MK acknowledges the Academy of Finland professor grant (no. 302958) and ATM-GTP European Research Council grant under the European Union's Horizon 2020 research and innovation program (no. 742206). OS, AS, SZ and JB acknowledge bilateral collaboration supported by Academy of Finland grant 314 798/799 and Russian Foundation for Basic Research grants 18-55-11005 and 19-17-00209. TP acknowledges Funding through Academy of Finland ('Natural Secreted Nano Vesicles as a Source of Novel Biomass Products for Circular Economy', NANOBIOMASS, 307537). KK was supported by the Academy of Finland (Academy Research Fellow project 294600).

References

Aakala, T., Hari, P., Dengel, S., Newberry, S. L., Mizunuma, T., and Grace, J.: A prominent stepwise advance of the tree line in north-east Finland, Journal of Ecology, 102, 1582–1591, 2014.

Barrett, K., Rocha, A. V., van de Weg, M. J., and Shaver, G.: Vegetation shifts observed in arctic tundra 17 years after fire, Remote Sensing Letters, 3, 729–736, 2012.

Beringer, J., Chapin III, F. S., Thompson, C. C., and McGuire, A. D.: Surface energy exchanges along a tundra-forest transition and feedbacks to climate, Agricultural and Forest Meteorology, 131, 143–161, 2005.

Bernes, C., Bråthen, K. A., Forbes, B. C., Speed, J. D., and Moen, J.: What are the impacts of reindeer/caribou (Rangifer tarandus L.) on arctic and alpine vegetation? A systematic review, Environmental Evidence, 4, 4, 2015.

Bjorkman, A. D., Criado, M. G., Myers-Smith, I. H., Ravolainen, V., Jónsdóttir, I. S., Westergaard, K. B., Lawler, J. P., Aronsson, M., Bennett, B., Gardfjell, H., et al.: Status and trends in Arctic vegetation: Evidence from experimental warming and long-term monitoring, Ambio, 49, 678–692, 2020.

Blaschke, T.: Object based image analysis for remote sensing, ISPRS journal of photogrammetry and remote sensing, 65, 2–16, 2010.

Bonan, G. B.: A computer model of the solar radiation, soil moisture, and soil thermal regimes in boreal forests, Ecological Modelling, 45, 275–306, 1989.

Box, J. E., Colgan, W. T., Christensen, T. R., Schmidt, N. M., Lund, M., Parmentier, F.-J. W., Brown, R., Bhatt, U. S., Euskirchen, E. S., Romanovsky, V. E., et al.: Key indicators of Arctic climate change: 1971–2017, Environmental Research Letters, 14, 045 010, 2019.

Bret-Harte, M. S., Mack, M. C., Shaver, G. R., Huebner, D. C., Johnston, M., Mojica, C. A., Pizano, C., and Reiskind, J. A.: The response of Arctic vegetation and soils following an unusually severe tundra fire, Philosophical Transactions of the Royal Society B: Biological Sciences, 368, 20120 490, 2013.

Camac, J. S., Williams, R. J., Wahren, C.-H., Hoffmann, A. A., and Vesk, P. A.: Climatic warming strengthens a positive feedback between alpine shrubs and fire, Global Change Biology, 23, 3249–3258, 2017.

Chorley, R. J.: Introduction to physical hydrology, London: Methuen, 1971.

Frost, G. V. and Epstein, H. E.: Tall shrub and tree expansion in Siberian tundra ecotones since the 1960s, Global Change Biology, 20, 1264–1277, 2014.

Hansen, M. C., Potapov, P. V., Moore, R., Hancher, M., Turubanova, S. A., Tyukavina, A., Thau, D., Stehman, S., Goetz, S. J., Loveland, T. R., et al.: High-resolution global maps of 21st-century forest cover change, Science, 342, 850–853, 2013.

Harsch, M. A. and Bader, M. Y.: Treeline form–a potential key to understanding treeline dynamics, Global Ecology and Biogeography, 20, 582–596, 2011.

Ilyina, I. S., Lapshina, E. I., Lavrenko, N. N., et al.: West Siberian Plain Vegetation Cover, 1985.

Johansen, B. and Tømmervik, H.: The relationship between phytomass, NDVI and vegetation communities on Svalbard, International Journal of Applied Earth Observation and Geoinformation, 27, 20–30, 2014.

Joly, K., Jandt, R. R., and Klein, D. R.: Decrease of lichens in Arctic ecosystems: the role of wildfire, caribou, reindeer, competition and climate in north-western Alaska, Polar Research, 28, 433–442, 2009.

Jones, B. M., Breen, A. L., Gaglioti, B. V., Mann, D. H., Rocha, A. V., Grosse, G., Arp, C. D., Kunz, M. L., and Walker, D. A.: Identification of unrecognized tundra fire events on the north slope of Alaska, Journal of Geophysical Research: Biogeosciences, 118, 1334–1344, 2013.

Kalliokoski, T., Aalto, T., Bäck, J., Ezhova, E., Franz, D., Haapanala, S., Juurola, E., Kerminen, V.-M., Kolari, P., Kulmala, L., et al.: Carbon
sink and CarbonSink+: from observations to global potential, 2019.

Kaplan, J. O. and New, M.: Arctic climate change with a 2°C global warming: Timing, climate patterns and vegetation change, Climatic
change, 79, 213–241, 2006.

Katsov, V., Semenov, S., Alekseev, G., Ananicheva, M., et al.: Second Roshydromet Assessment Report on Climate Change and its Conse-
quences in the Russian Federation, Moscow, Roshydromet, 2014.

Kharuk, V. I., Ranson, K. J., Dvinskaya, M. L., and Im, S. T.: Wildfires in northern Siberian larch dominated communities, Environmental
Research Letters, 6, 045 208, 2011.

Köster, E., Köster, K., Aurela, M., Laurila, T., Berninger, F., Lohila, A., and Pumpanen, J.: Impact of reindeer herding on vegetation biomass
and soil carbon content: a case study from Sodankylä, Finland., Boreal Environment Research, 2013.

Köster, E., Köster, K., Berninger, F., Prokushkin, A., Aaltonen, H., Zhou, X., and Pumpanen, J.: Changes in fluxes of carbon dioxide and
methane caused by fire in Siberian boreal forest with continuous permafrost, Journal of environmental management, 228, 405–415, 2018.

Kukkonen, I. T., Suhonen, E., Ezhova, E., Lappalainen, H., Gennadinik, V., Ponomareva, O., Gravis, A., Miles, V., Kulmala, M., Melnikov,
V., et al.: Observations and modelling of ground temperature evolution in the discontinuous permafrost zone in Nadym, north-west Siberia,
Permafrost and Periglacial Processes, 2020.

Kulmala, M.: Build a global Earth observatory, Nature, 553, 21–23, 2018.

Kulmala, M., Nieminen, T., Chellapermal, R., Makkonen, R., Bäck, J., and Kerminen, V.-M.: Climate feedbacks linking the increasing
atmospheric CO_2 concentration, BVOC emissions, aerosols and clouds in forest ecosystems, in: Biology, controls and models of tree
volatile organic compound emissions, pp. 489–508, Springer, 2013.

Kulmala, M., Lappalainen, H. K., Petäjä, T., Kurten, T., Kerminen, V.-M., Viisanen, Y., Hari, P., Sorvari, S., Bäck, J., Bondur, V., Kasimov, N.,
Kotlyakov, V., Matvienko, G., Baklanov, A., Guo, H. D., Ding, A., Hansson, H.-C., and Zilitinkevich, S.: Introduction: The Pan-Eurasian
Experiment (PEEX) - multidisciplinary, multiscale and multicomponent research and capacity-building initiative, Atmospheric Chemistry
and Physics, 15, 13 085–13 096, https://doi.org/10.5194/acp-15-13085-2015, https://www.atmos-chem-phys.net/15/13085/2015/, 2015.

Landhausser, S. M. and Wein, R. W.: Postfire vegetation recovery and tree establishment at the Arctic treeline: climate-change-vegetation-
response hypotheses, Journal of Ecology, pp. 665–672, 1993.

Lantz, T. C., Marsh, P., and Kokelj, S. V.: Recent shrub proliferation in the Mackenzie Delta uplands and microclimatic implications,
Ecosystems, 16, 47–59, 2013.

Lappalainen, H. K., Kerminen, V.-M., Petäjä, T., Kurten, T., Baklanov, A., Shvidenko, A., Bäck, J., Vihma, T., Alekseychik, P., Andreae,
M. O., Arnold, S. R., Arshinov, M., Asmi, E., Belan, B., Bobylev, L., Chalov, S., Cheng, Y., Chubarova, N., de Leeuw, G., Ding, A.,
Dobrolyubov, S., Dubtsov, S., Dyukarev, E., Elansky, N., Eleftheriadis, K., Esau, I., Filatov, N., Flint, M., Fu, C., Glezer, O., Gliko, A.,
Heimann, M., Holtslag, A. A. M., Hõrrak, U., Janhunen, J., Juhola, S., Järvi, L., Järvinen, H., Kanukhina, A., Konstantinov, P., Kotlyakov,
V., Kieloaho, A.-J., Komarov, A. S., Kujansuu, J., Kukkonen, I., Duplissy, E.-M., Laaksonen, A., Laurila, T., Lihavainen, H., Lisitzin,
A., Mahura, A., Makshtas, A., Mareev, E., Mazon, S., Matishov, D., Melnikov, V., Mikhailov, E., Moisseev, D., Nigmatulin, R., Noe,
S. M., Ojala, A., Pihlatie, M., Popovicheva, O., Pumpanen, J., Regerand, T., Repina, I., Shcherbinin, A., Shevchenko, V., Sipilä, M.,
Skorokhod, A., Spracklen, D. V., Su, H., Subetto, D. A., Sun, J., Terzhevik, A. Y., Timofeyev, Y., Troitskaya, Y., Tynkkynen, V.-P.,
Kharuk, V. I., Zaytseva, N., Zhang, J., Viisanen, Y., Vesala, T., Hari, P., Hansson, H. C., Matvienko, G. G., Kasimov, N. S., Guo, H.,
Bondur, V., Zilitinkevich, S., and Kulmala, M.: Pan-Eurasian Experiment (PEEX): towards a holistic understanding of the feedbacks and

interactions in the land–atmosphere–ocean–society continuum in the northern Eurasian region, Atmospheric Chemistry and Physics, 16, 14 421–14 461, https://doi.org/10.5194/acp-16-14421-2016, 2016.

MacDonald, G., Kremenetski, K., and Beilman, D.: Climate change and the northern Russian treeline zone, Philosophical Transactions of the Royal Society B: Biological Sciences, 363, 2283–2299, 2008.

515 Maliniemi, T., Kapfer, J., Saccone, P., Skog, A., and Virtanen, R.: Long-term vegetation changes of treeless heath communities in northern Fennoscandia: Links to climate change trends and reindeer grazing, Journal of Vegetation Science, 29, 469–479, 2018.

Matveev, A. A. and Musaev, R. A.: Preservation of the ecological balance in the context of the economic development of Yamal-Nenets Autonomous district, in: Proceedings of the international conference 'Economy and modern Management: Theory and Practice', p. 33436, Novosibirsk, 2013.

520 Matyshak, G., Bogatyrev, L., Goncharova, O. Y., and Bobrik, A.: Specific features of the development of soils of hydromorphic ecosystems in the northern taiga of Western Siberia under conditions of cryogenesis, Eurasian Soil Science, 50, 1115–1124, 2017a.

Matyshak, G., Goncharova, O. Y., Moskalenko, N., Walker, D., Epstein, H., and Shur, Y.: Contrasting soil thermal regimes in the Forest-tundra transition near Nadym, West Siberia, Russia, Permafrost and Periglacial Processes, 28, 108–118, 2017b.

Mekonnen, Z. A., Riley, W. J., Randerson, J. T., Grant, R. F., and Rogers, B. M.: Expansion of high-latitude deciduous forests driven by

525 interactions between climate warming and fire, Nature plants, 5, 952–958, 2019.

Miles, V. V. and Esau, I.: Spatial heterogeneity of greening and browning between and within bioclimatic zones in northern West Siberia, Environmental Research Letters, 11, 115 002, 2016.

Myers-Smith, I. H. and Hik, D. S.: Climate warming as a driver of tundra shrubline advance, Journal of Ecology, 106, 547–560, 2018.

Myers-Smith, I. H., Grabowski, M. M., Thomas, H. J., Angers-Blondin, S., Daskalova, G. N., Bjorkman, A. D., Cunliffe, A. M., Assmann,

530 J. J., Boyle, J. S., McLeod, E., et al.: Eighteen years of ecological monitoring reveals multiple lines of evidence for tundra vegetation change, Ecological Monographs, 89, e01 351, 2019.

Myers-Smith, I. H., Kerby, J. T., Phoenix, G. K., Bjerke, J. W., Epstein, H. E., Assmann, J. J., John, C., Andreu-Hayles, L., Angers-Blondin, S., Beck, P. S., et al.: Complexity revealed in the greening of the Arctic, Nature Climate Change, 10, 106–117, 2020.

Narita, K., Harada, K., Saito, K., Sawada, Y., Fukuda, M., and Tsuyuzaki, S.: Vegetation and permafrost thaw depth 10 years after a tundra

535 fire in 2002, Seward Peninsula, Alaska, Arctic, Antarctic, and Alpine Research, 47, 547–559, 2015.

Olofsson, J., Oksanen, L., Callaghan, T., Hulme, P. E., Oksanen, T., and Suominen, O.: Herbivores inhibit climate-driven shrub expansion on the tundra, Global Change Biology, 15, 2681–2693, 2009.

Petäjä, T., Ganzei, K., Lappalainen, H. K., Tabakova, K., Makkonen, R., Räisänen, J., Chalov, S., Kulmala, M., Zilitinkevich, S., Baklanov, P., Shakirov, R. B., Mishina, N. V.and Egidarev, E. G., and Kondrat'ev, I. I.: Research agenda for the Russian Far East and utilization of

540 multi-platform comprehensive environmental observations, Int. J. Digital Earth, submitted, 2020.

Ponomarev, E. I., Kharuk, V. I., and Ranson, K. J.: Wildfires dynamics in Siberian larch forests, Forests, 7, 125, 2016.

Post, E. and Pedersen, C.: Opposing plant community responses to warming with and without herbivores, Proceedings of the National Academy of Sciences, 105, 12 353–12 358, 2008.

Priestley, C. H. B. and Taylor, R.: On the assessment of surface heat flux and evaporation using large-scale parameters, Monthly weather

545 review, 100, 81–92, 1972.

Pulliainen, J., Aurela, M., Laurila, T., Aalto, T., Takala, M., Salminen, M., Kulmala, M., Barr, A., Heimann, M., Lindroth, A., et al.: Early snowmelt significantly enhances boreal springtime carbon uptake, Proceedings of the National Academy of Sciences, 114, 11 081–11 086, 2017.

Renwick, K. M. and Rocca, M. E.: Temporal context affects the observed rate of climate-driven range shifts in tree species, Global Ecology and Biogeography, 24, 44–51, 2015.

Rocha, A. V. and Shaver, G. R.: Postfire energy exchange in arctic tundra: the importance and climatic implications of burn severity, Global Change Biology, 17, 2831–2841, 2011.

Ruffner, K. C.: Corona: America's first satellite program, History Staff, Center for the Study of Intelligence, Central Intelligence Agency, 1995.

Sand, M., Berntsen, T., von Salzen, K., Flanner, M., Langner, J., and Victor, D. G.: Response of Arctic temperature to changes in emissions of short-lived climate forcers, Nature Climate Change, 6, 286–289, 2016.

Sannikov, S. et al.: Survival and growth of seedlings of conifer species in different types of micro-environment on felled areas., Ekologiya, pp. 60–68, 1970.

Sizov, O. S. and Lobotrosova, S. A.: Features of revegetation of sand blowout sites in the northern taiga subzone of Western Siberia, Earth Cryosphere, XX, 3–13, 2016.

Tchebakova, N. M., Monserud, R. A., and Nazimova, D. I.: A Siberian vegetation model based on climatic parameters, Canadian Journal of Forest Research, 24, 1597–1607, 1994.

Tchebakova, N. M., Parfenova, E. I., and Soja, A. J.: Potential climate-induced vegetation change in Siberia in the twenty-first century, in: Environmental Change in Siberia, pp. 67–82, Springer, 2010.

Trofimova, I. E. and Balybina, A. S.: Regionalization of the West Siberian Plain from thermal regime of soils, Geography and Natural Resources, 36, 234–244, 2015.

Van Bogaert, R., Haneca, K., Hoogesteger, J., Jonasson, C., De Dapper, M., and Callaghan, T. V.: A century of tree line changes in sub-Arctic Sweden shows local and regional variability and only a minor influence of 20th century climate warming, Journal of Biogeography, 38, 907–921, 2011.

Vermote, E., Justice, C., Claverie, M., and Franch, B.: Preliminary analysis of the performance of the Landsat 8/OLI land surface reflectance product, Remote Sensing of Environment, 185, 46–56, 2016.

Walker, D., Epstein, H., Jia, G., Balser, A., Copass, C., Edwards, E., Gould, W., Hollingsworth, J., Knudson, J., Maier, H., et al.: Phytomass, LAI, and NDVI in northern Alaska: Relationships to summer warmth, soil pH, plant functional types, and extrapolation to the circumpolar Arctic, Journal of Geophysical Research: Atmospheres, 108, 2003.

Walker, D. A., Raynolds, M. K., Daniëls, F. J., Einarsson, E., Elvebakk, A., Gould, W. A., Katenin, A. E., Kholod, S. S., Markon, C. J., Melnikov, E. S., et al.: The circumpolar Arctic vegetation map, Journal of Vegetation Science, 16, 267–282, 2005.

Walvoord, M. A., Voss, C. I., Ebel, B. A., and Minsley, B. J.: Development of perennial thaw zones in boreal hillslopes enhances potential mobilization of permafrost carbon, Environmental Research Letters, 14, 015 003, 2019.

Woodward, F. I., Lomas, M. R., and Kelly, C. K.: Global climate and the distribution of plant biomes, Philosophical Transactions of the Royal Society of London. Series B: Biological Sciences, 359, 1465–1476, 2004.

Zhu, K., Woodall, C. W., and Clark, J. S.: Failure to migrate: lack of tree range expansion in response to climate change, Global Change Biology, 18, 1042–1052, 2012.
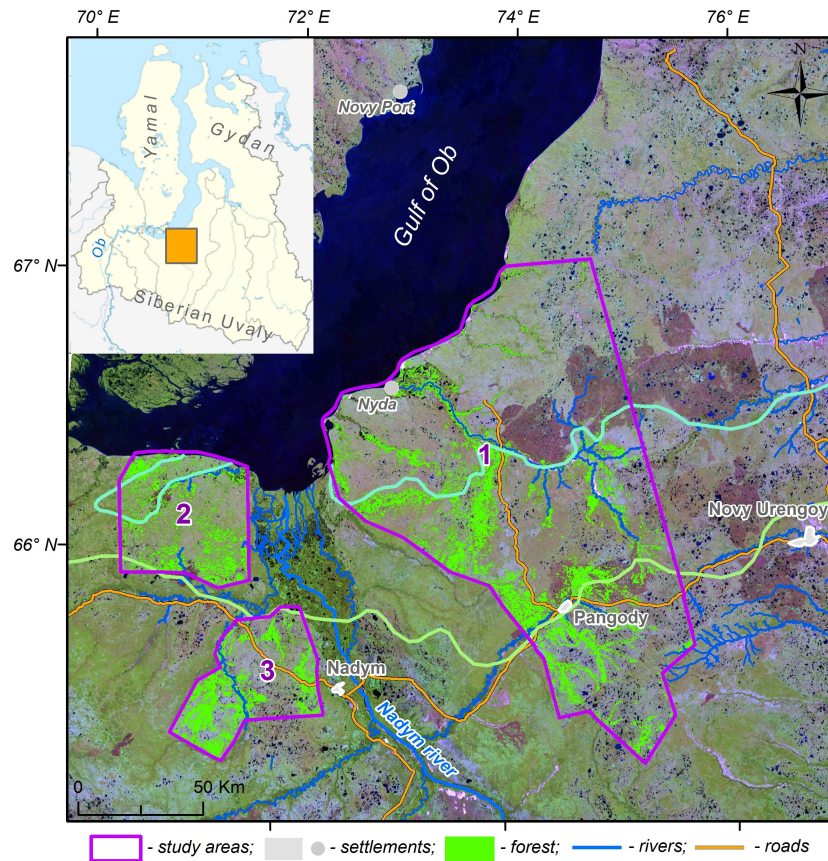
Figure 1. Study areas 1, 2 and 3 are shown in the Landsat-7 mosaic (2001). Green areas display the forest mask obtained from the topographic map (Ilyina et al., 1985). Cyan curve is the boundary between southern tundra and tundra-forest ecotone, light green curve is the boundary between forest-tundra ecotone and northern taiga (Ilyina et al., 1985). Inset: orange rectangular region marks the location of the study sites on the map of Yamal-Nenets Autonomous District.

Figure 2. Illustration of vegetation cover in the photos from the field campaign: the background site (left panel) and the nearby site affected by fires before 1968 and 1988 (right panel).
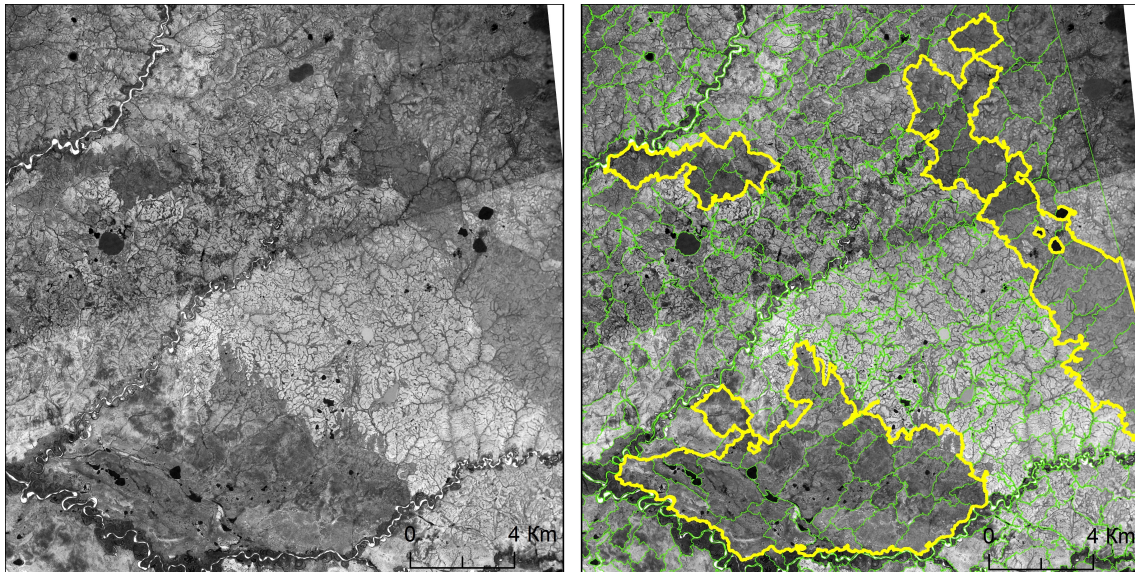
Figure 3. An example of segmentation and classification of burned areas in Corona mosaic. Left panel: original mosaic. Right panel: mosaic after segmentation and classification. Green curves - boundaries of segments, yellow curves - boundaries of identified burned areas.
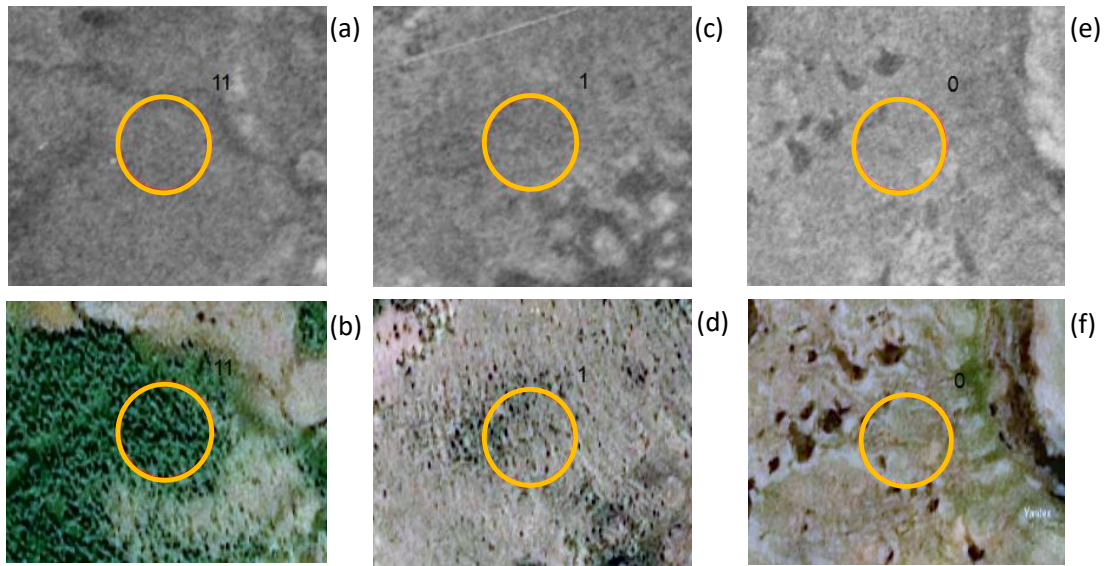
Figure 4. Examples of samples used for the visual analysis of vegetation dynamics. Diameter of each sample is 100 m. Images are taken from 'Corona' mission and SPOT-6,7 (©Yandex.Maps). (a)-(b): shift to forest, (c)-(d): shift to woodlands, (e)-(f): no shift.
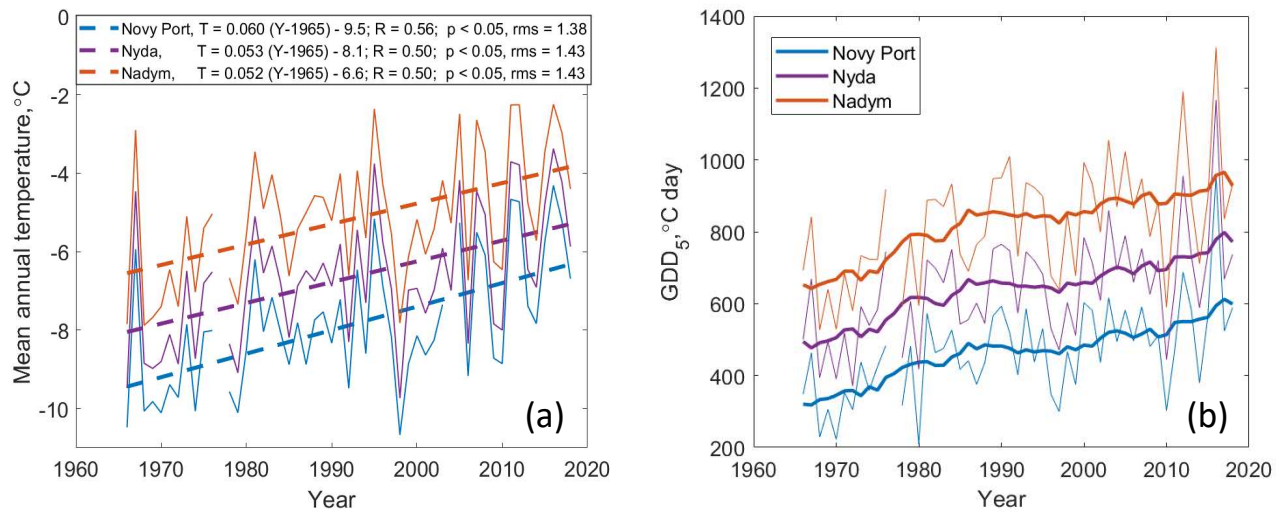
Figure 5. (a) Time series of mean annual temperature (solid) and corresponding linear fits (dashed). In the legend, T is the mean annual temperature and Y is the year. (b) Time series of growing degree-days (thin solid curves) and 10-yr running average (thick solid curves)

.
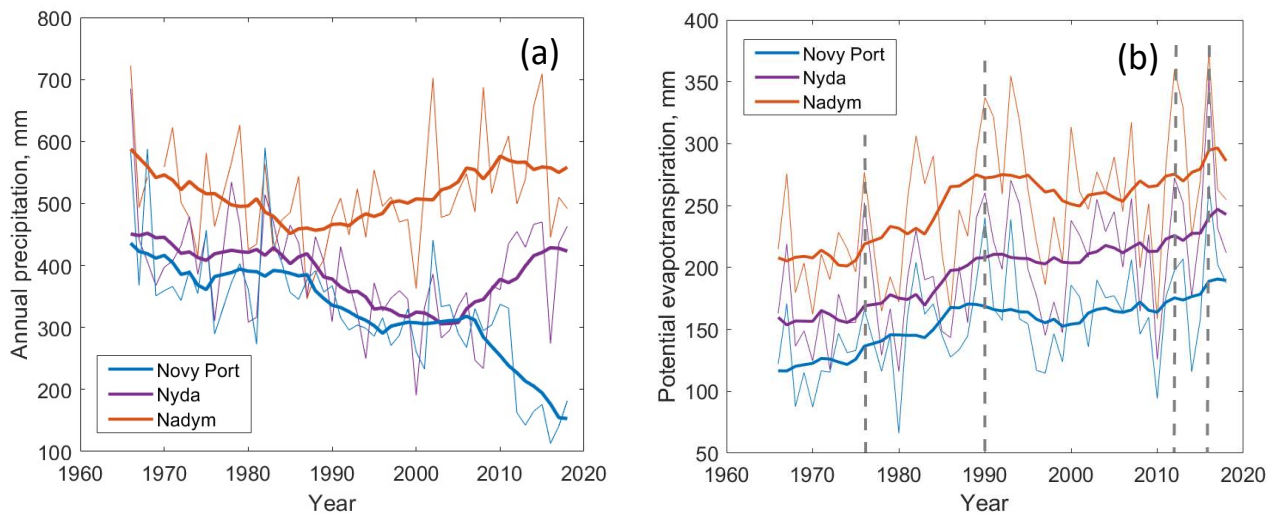
Figure 6. (a) Time series of annual precipitation and (b) potential evapotranspiration. Thick curves correspond to 10-yr running average. Dashed lines in panel (b) mark the years of major fires.
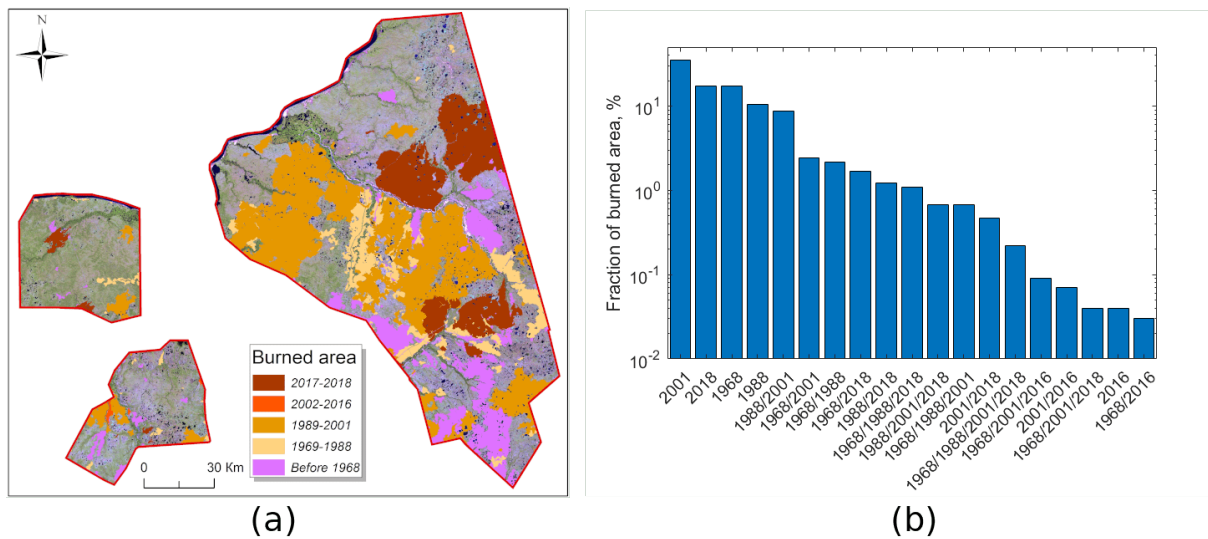
Figure 7. (a) Burned territories within study areas 1, 2 and 3. (b) The fraction of burned area defined as the burned area in the mosaic from particular year(s) divided by the total burned area during the whole study period. Multiple years in x-axis correspond to multiple fires at the same site.
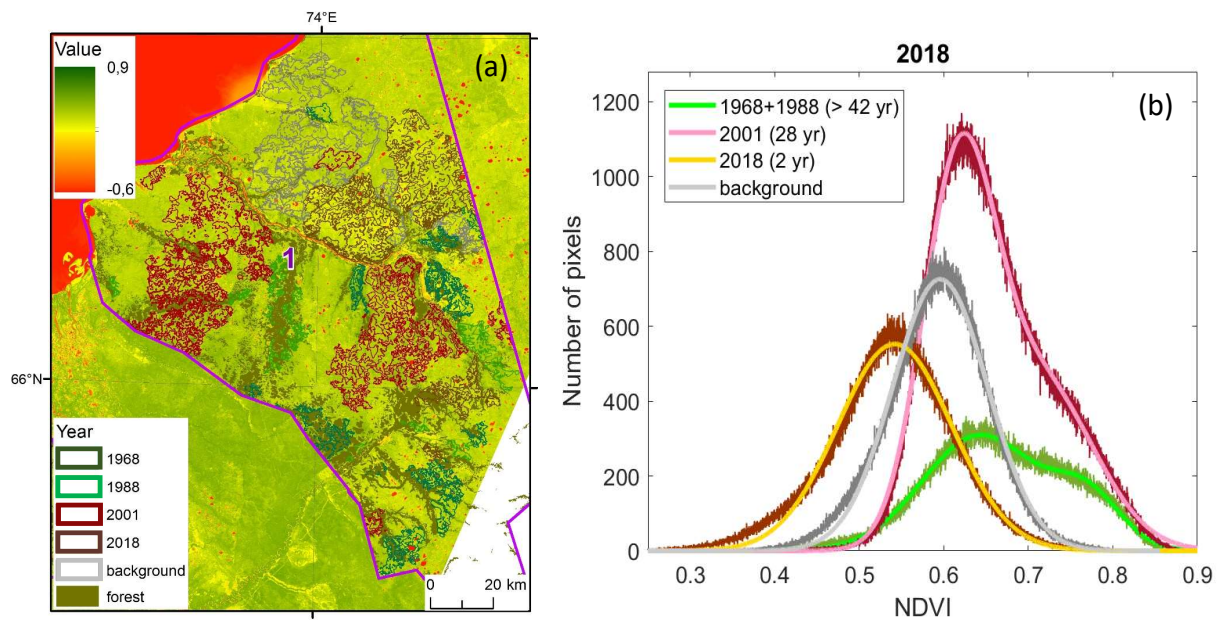
Figure 8. (a) The distribution of NDVI over study area 1 on 30 June 2018. Segments with boundaries of different color are background dry tundra sites and burned dry tundra sites detected in Corona and Landsat mosaics from different years (see legend). Burned areas in the mosaics from 1968 and 1988 are mainly due to fires from >42 years ago, in 2001 – due to fires from 28 years ago, in 2018 – due to fires from 2 years ago. (b) Distributions of NDVI based on the data from marked background sites and sites burned in different years. In the legend, numbers in brackets indicate years after the last major fire.
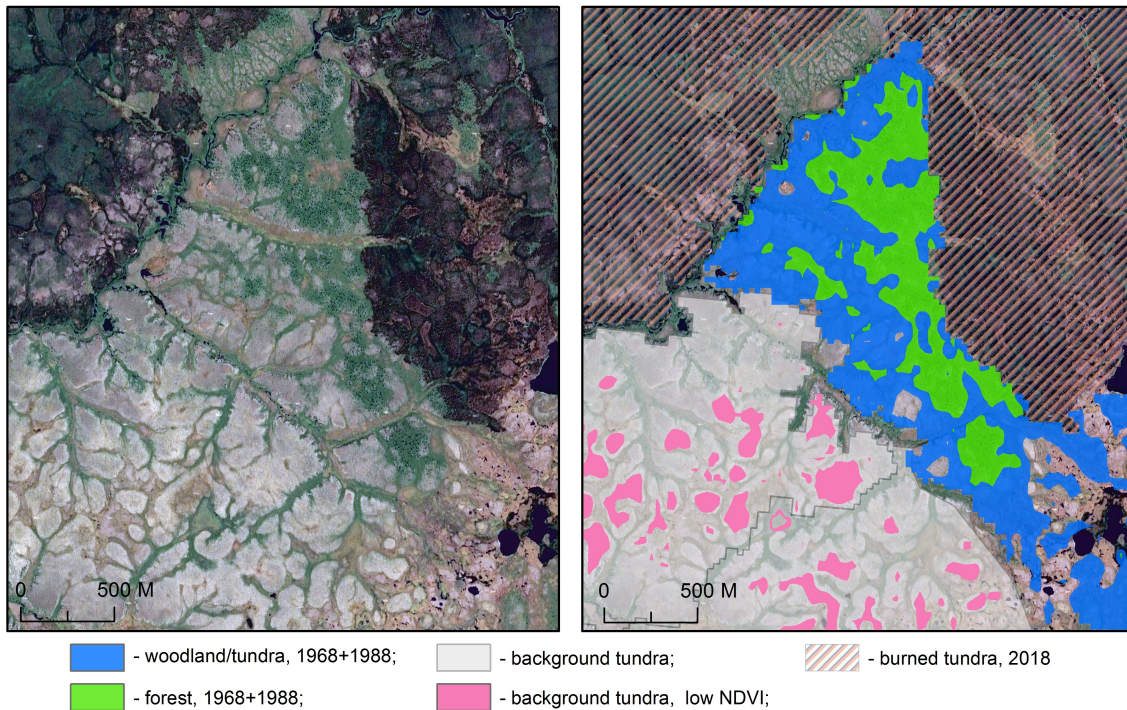
Figure 9. Representative types of vegetation associated with different state of the sites and NDVI. Left panel: an image without mask, right panel: the same image colored according to the state of the site (burned in mosaics from 1968+1988 or 2018, background) and to NDVI. Right panel: green color corresponds to the upper peak and blue color corresponds to the lower peak in the bimodal distribution from the sites burned before 1968 and 1988 (Fig. 8b). Pink color marks pixels with NDVI lower than 0.52 in the background site.
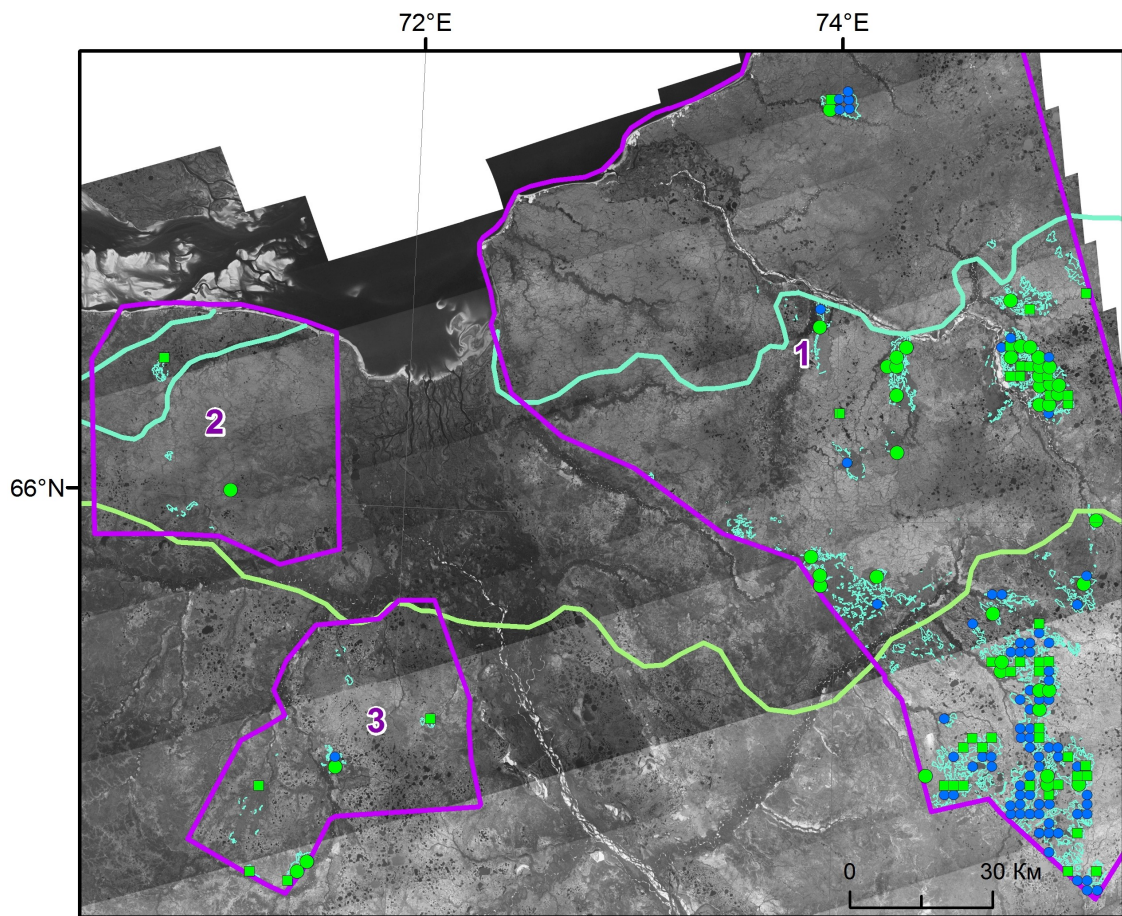
Figure 10. Illustration of the vegetation shift in dry tundra after the fire (time interval ca 60 years). Blue circles – no shift, green squares – shift to woodlands, green circles – shift to forest. Cyan curve is the boundary between southern tundra and forest-tundra, green curve is the boundary between forest-tundra and northern taiga (source: topographic maps).
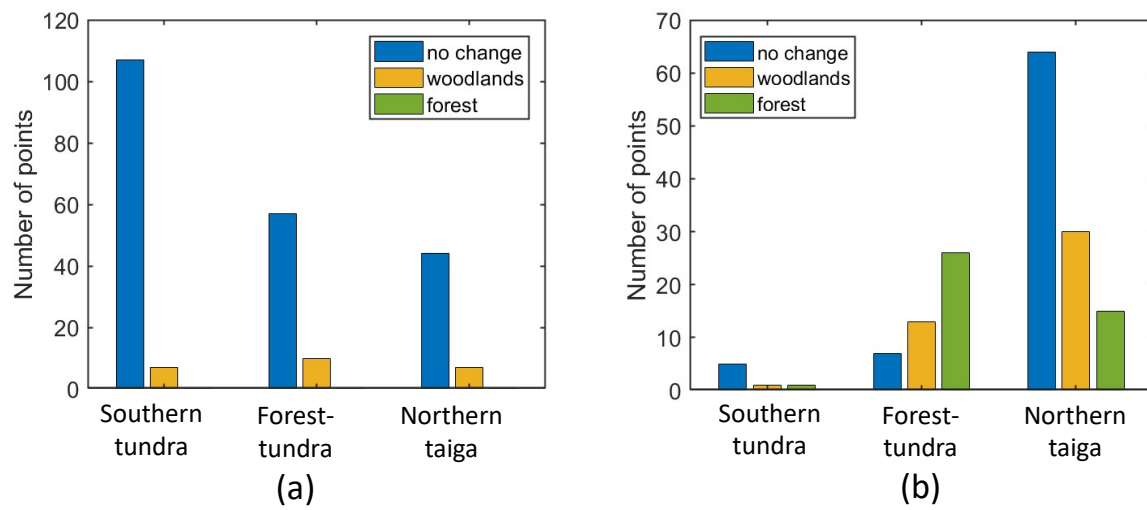
Figure 11. (a) Number of checkpoints for different vegetation classes, background territories. (b) Number of checkpoints for different vegetation classes, fire-affected territories. The time interval is ca 60 years.
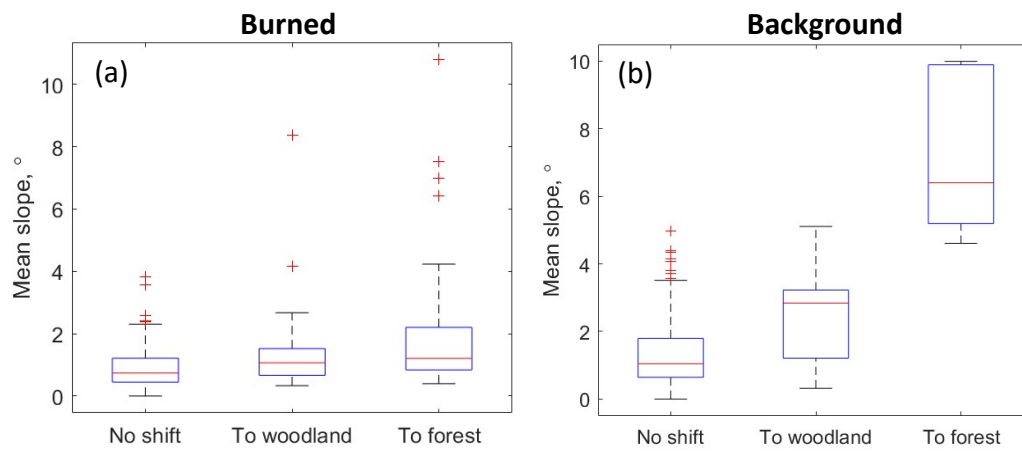
Figure 12. Median boxplots of the mean topographic slopes within the check circles. Red line - median values, bottom and top edges of boxes – 25th and 75th percentiles, whiskers 5th and 95th percentiles and red crosses - outliers.

Table 1. Description of the study areas. Classification of the study areas according to vegetation types.

Study area	Location	Surface area (km^2)	Vegetation distribution (Ilyina et al., 1985)
1	triangle with vertices at (65°17'N 75°12'E), (66°30'N 72°05'E) and (67°06'N 74°40'E)	15800	ca 50% of dry and wet tundra (mainly northern part), 10-15% of woodlands along the rivers, 30-35% of northern taiga wetlands (mainly southern part) small areas (< 3%) along the rivers are covered by forests
2	quadrangle with vertices at (66°19'N 71°00'E), (65°55'N 71°42'E), (65°55'N 70°34'E) and (66°19'N 70°23'E)	2500	>50% of woodlands, ca 20% in the north –dry and wet tundra ca 5% in the south – northern taiga
3	quadrangle with vertices at (65°49'N 72°07'E), (65°26'N 72°23'E), (65°15'N 71°32'E) and (65°21'N 71°05'E)	2000	20% – woodlands, 30-40% - northern taiga wetlands, 30-40% northern taiga forests.

Table 2. Field observations of vegetation and active layer thickness

Site	Active layer thickness (cm)	Vegetation cover
65°50'59.49"N, 74°23'03.91"E – background	38.3 (min 38, max 40, n=3)	lichen (*Cladonia alpestris, Cladonia rangiferina, Cetraria nivalis*) – up to 40%, shrubs (*Betula nana, Ledum*) – up to 70%, cloudberry (*Rubus chamaemorus*) – up to 5%
65°50'51.14"N 74°24'58.39"E – fire before 1968 and 1988	119.0 (min 90, max 170, n=10)	lichen (*Cladonia alpestris, Cladonia rangiferina, Cetraria nivalis*) – up to 60%, shrubs (*Betula nana, Ledum, Vaccínium uliginósum*) – up to 80%, mosses (*Polytrichum*) – up to 50%
65°56'18.27"N 74°38'59.00"E – fire before 1988	102.0 (min 70, max 130, n=5)	lichen (*Cladonia alpestris, Cladonia rangiferina, Cetraria nivalis*) – up to 20%, shrubs (*Betula nana, Ledum, Vaccínium uliginósum*) – up to 70%, mosses (*Polytrichum*) – up to 30%

Table 3. Classification of vegetation classes based on growing degree-days (GDD_5) and dryness index (DI) (Tchebakova et al., 1994)

Vegetation class	GDD_5 (°C day)	DI
Tundra	0-300	< 3.3
Spruce-larch forest – tundra	300-500	< 2.0
Dark-needled northern taiga	500-800	< 2.3
Dark-needled northern taiga	800-1000	< 2.3

Table 4. Data sets used for fire analysis

Data set	Source	Date	Path/Row	Resolution
Landsat-5		1987-1988	159/013, 159/014, 161/013, 161/014	30 m
Landsat-7		2000-2002	159/013, 159/014, 161/013, 161/014	30 m
Landsat-8	US Geological Survey[1]	2016	159/013, 159/014, 160/013, 160/014, 161/013, 161/014	30 m
Landsat-8		2017-2018	159/013, 159/014, 160/014, 161/013, 161/014	30 m
Landsat-8		2019	160/013, 160/014	30 m

[1] https://apps.sentinel-hub.com/sentinel-playground

Table 5. Relations between Landsat mosaic years and the years of major fires

Satellite image year	1968	1988	2001	2016	2018
Preceding major fire year	between 1953[1] and 1964[2]	1976[2]	1990[3]	2012[3]	2016[3]

[1] Chekunova V.S., Geological and geomorfological survey of a part of the lower reaches of the River Nadym basin and parts of the right bank of the River Ob in Nadym region in 1953. VSEGEI: 1954. 72 p.

[2] Corona images, https://earthexplorer.usgs.gov

[3] Landsat images, https://apps.sentinel-hub.com/sentinel-playground

Table 6. Data sets used for the analysis of vegetation dynamics

Data set	Source	Date	Path/ map sheet number	Resolution
Corona/KH-4b	US Geological Survey[1]	21.08.1968	DS1104-2217DA(24...45)	≈ 2 m
'Resurs-P' 1,2	Roscosmos[2]	07.11.2016 04.07.2016 28.09.2016	7081_05 8513_02 9830_01	1.6 m
SPOT-6,7	YandexMaps/ AirbusDS[3]	2016-2017	-	1.5 m
Digital elevation model ArcticDEM, v. 3.0	National Geographic Agency, US[4]	2018 (survey 2010-2017)	52_63_2_2, 52_64_1_1, 52_64_1_2, 52_64_2_2, 52_64_2_1, 52_65_1_2, 53_62_2_1, 53_62_2_2, 53_63_2_2, 53_63_1_1, 53_63_1_2, 53_63_2_1, 53_64_2_1, 53_64_1_2, 53_64_1_1, 53_65_1_1, 54_63_2_2, 54_63_2_1, 54_63_1_1, 54_64_1_2, 54_64_1_1	2 m
Topographic maps	Rosreestr[5], Ilyina et al., 1985, Supplementary material	1968-1971	Q-42-57,58; Q-42-59,60; Q-42-69,70; Q-42-71,72; Q-42-81,82; Q-42-83,84; Q-42-95,96; Q42-107,108; Q-43-27,28; Q-43-29,30; Q-43-37,38; Q-43-39,40; Q-43-41,42; Q-43-43,44; Q-43-49,50; Q-43-51,52; Q-43-53,54; Q-43-55,56; Q-43-61,62; Q-43-63,64; Q-43-65,66; Q-43-67,68; Q-43-73,74; Q-43-75,76; Q-43-77,78; Q-43-79,80; Q-43-85,86; Q-43-89,90; Q-43-91,92; Q-43-103,104	1:100 000
NDVI Landsat	US Geological Survey[1]	30.06.2018	160/014-160/013	30 m

[1] https://earthexplorer.usgs.gov

[2] https://gptl.ru

[3] https://yandex.ru/maps

[4] https://arctic-nga.opendata.arcgis.com

[5] https://www.marshruty.ru/Maps/Maps.aspx

Table 7. Best fit parameters of the NDVI distributions in Fig. 8b by the function $N_{pix} = A_1 \exp(-\frac{(NDVI - NDVI_{max,1})^2}{2\sigma_1^2}) + A_2 \exp(-\frac{(NDVI - NDVI_{max,2})^2}{2\sigma_2^2})$

Year	A_1	$NDVI_{max,1}$	σ_1	A_2	$NDVI_{max,2}$	σ_2
1968+1988	308	0.64	0.07	132	0.77	0.04
2001	954	0.62	0.04	448	0.71	0.06
2018	552	0.54	0.07	-	-	-
Background	726	0.59	0.06	-	-	-

Table 8. Number of checkpoints (percentage of all checkpoints within a vegetation class, %) corresponding to vegetation shift in fire-affected and background dry tundra

State of vegetation	South tundra, fires	Forest-tundra, fires	Northern taiga, fires	South tundra, background	Forest-tundra, background	Northern taiga, background
No shift	5 (71.6)	7 (15.2)	64 (58.7)	107 (93.9)	57 (85.1)	44 (86.3)
To woodlands	1 (14.3)	13 (28.3)	30 (27.5)	7 (6.1)	10 (14.9)	7 (13.7)
To forests	1 (14.3)	26 (56.5)	15 (13.8)	0 (0)	0 (0)	0 (0)
All	7 (100)	46 (100)	109 (100)	114 (100)	67 (100)	51 (100)
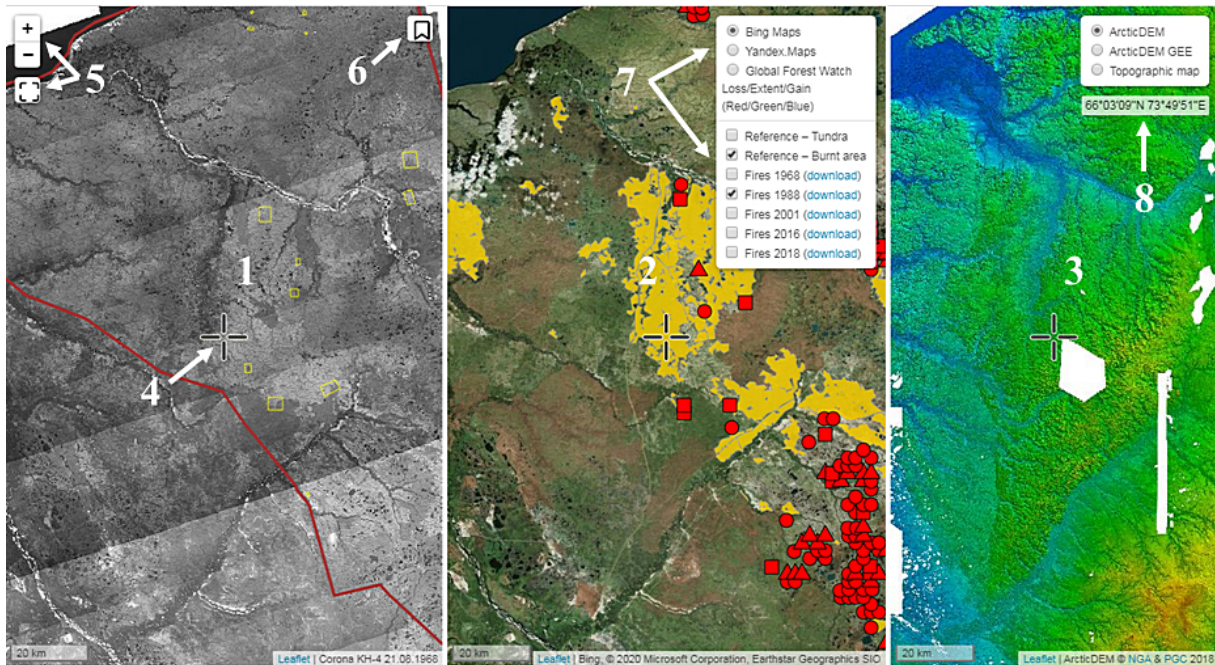
Figure A1. Interface of geoportal NC 50: 1 – map 1; 2 – map 2; 3 – map 3; 4 – map pointer; 5 – zoom; 6 – widget containing bookmarks of the reference sites; 7 – panel of base maps and layers; 8 – current coordinates.